First lasing and operation of an Ångstrom-wavelength free-electron laser

Article *in* Nature Photonics · August 2010

DOI: 10.1038/nphoton.2010.176 · Source: OAI

nature photonics

ARTICLES

PUBLISHED ONLINE: 1 AUGUST 2010 | DOI: 10.1038/NPHOTON.2010.176

First lasing and operation of an ångstrom-wavelength free-electron laser

P. Emma[1]*, R. Akre[1], J. Arthur[1], R. Bionta[2], C. Bostedt[1], J. Bozek[1], A. Brachmann[1], P. Bucksbaum[1], R. Coffee[1], F.-J. Decker[1], Y. Ding[1], D. Dowell[1], S. Edstrom[1], A. Fisher[1], J. Frisch[1], S. Gilevich[1], J. Hastings[1], G. Hays[1], Ph. Hering[1], Z. Huang[1], R. Iverson[1], H. Loos[1], M. Messerschmidt[1], A. Miahnahri[1], S. Moeller[1], H.-D. Nuhn[1], G. Pile[3], D. Ratner[1], J. Rzepiela[1], D. Schultz[1], T. Smith[1], P. Stefan[1], H. Tompkins[1], J. Turner[1], J. Welch[1], W. White[1], J. Wu[1], G. Yocky[1] and J. Galayda[1]

The recently commissioned Linac Coherent Light Source is an X-ray free-electron laser at the SLAC National Accelerator Laboratory. It produces coherent soft and hard X-rays with peak brightness nearly ten orders of magnitude beyond conventional synchrotron sources and a range of pulse durations from 500 to <10 fs (10^{-15} s). With these beam characteristics this light source is capable of imaging the structure and dynamics of matter at atomic size and timescales. The facility is now operating at X-ray wavelengths from 22 to 1.2 Å and is presently delivering this high-brilliance beam to a growing array of scientific researchers. We describe the operation and performance of this new 'fourth-generation light source'.

Over the past several decades, intense beams of X-rays from synchrotron light sources have been used quite successfully to reveal the arrangement of atoms in a wide range of materials, including semiconductors, polymers, ceramics and biological molecules. Unlike visible light, X-ray wavelengths are comparable to the interatomic spacings in matter, thus enabling imaging on the atomic scale. However, even so-called 'third-generation' synchrotron sources produce insufficient brightness to resolve the structure of isolated single molecules. Synchrotrons also generate picoseconds-long X-ray pulses, which yield only blurred images of atoms and molecules in motion. In addition, accelerator research[1] has been focused for some time on advancements in applications of accelerators towards coherent emission from a bunch of electrons. These motivations, along with the desire to invent an X-ray laser, have led to the development a 'fourth-generation light source' based on the free-electron laser (FEL).

A FEL[2] is a source of coherent radiation that uses the interaction between an electromagnetic wave and a bunch of relativistic electrons to amplify this wave as the electrons pass through a periodic magnetic array (an undulator). In principle, the FEL wavelength is tunable from the far-infrared to hard X-rays and, similar to a conventional laser, the FEL can be configured as either an amplifier or an oscillator. At X-ray wavelengths, the simplest arrangement is the so-called self-amplified spontaneous emission (SASE)[3,4], a process that amplifies radiation from the electron shot noise in a long undulator to produce coherent X-rays of extremely high brightness. The radiated power develops exponentially along the undulator, with the gain length L_G defined as the distance over which the power increases by $e \approx 2.72$. The gain length depends critically on the transverse emittance ϵ (the intrinsic beam volume in phase space) of the electron beam, and its peak current I_{pk}. In one-dimensional theory[4,5] the relationship is given as $L_G \propto (\varepsilon/I_{pk})^{1/3}$.

A high peak current (typically kiloamp levels) and an emittance on the order of the X-ray wavelength will provide a reasonable gain length with power saturation after 18–20 gain lengths, providing stability of the shot-to-shot FEL power against small variations of the electron beam brightness.

The Linac Coherent Light Source (LCLS)[6,7], first proposed[8] in 1992, is such a light source, with ultrafast pulse durations on the femtosecond timescale[9]. It allows the imaging of single molecules and, working like a high-speed camera, also enables the creation of molecular movies, potentially revealing the details of physical, chemical and biological dynamics on an unprecedented timescale[10].

The principles of the SASE FEL have been demonstrated at longer wavelengths[11–16], and the FLASH facility in Hamburg in Germany currently operates such a SASE FEL at wavelengths down to 65 Å (ref. 17). Several hard-X-ray machines have either been proposed or are under construction[18–20], but the LCLS is the first hard-X-ray FEL in operation and has served users since 1 October 2009. The performance and operation of the LCLS are described here, beginning with a list of typical measured and design parameters (Table 1) for both soft and hard X-ray settings. The X-ray wavelength is easily tunable from 22 to 1.2 Å by varying the electron energy in the range 3.5–15 GeV.

The pulse repetition rate is presently limited to 30 Hz, but will be increased to 120 Hz later in 2010. In addition to these parameter sets, a new low-charge mode of operation (20 pC) has been developed that now produces X-ray pulse lengths of less than 10 fs full-width at half-maximum (FWHM)[21] with 0.1–0.2 mJ per pulse at any desired wavelength in the range 1.2–22 Å.

Electron source and linear accelerator

To drive an FEL at hard-X-ray wavelengths, a high-energy, exceptionally bright electron beam is required, where the brightness is engendered in its six-dimensional phase space density. A high-energy linear accelerator, with an appropriate injector and careful beam brightness preservation, can generate and deliver beam brightness levels more than 1,000 times higher than standard storage rings.

[1]SLAC National Accelerator Laboratory, Stanford, California 94309, USA, [2]Lawrence Livermore National Laboratory, Livermore, California 94550, USA, [3]Argonne National Laboratory, Argonne, Illinois 60439, USA. *e-mail: emma@slac.stanford.edu

Table 1 | Design and typical measured parameters for both hard (8.3 keV) and soft (0.8–2.0 keV) X-rays. The 'design' and 'hard' values are shown only at 8.3 keV. Stability levels are measured over a few minutes.

Parameter	Design	Hard	Soft	Unit
Electrons				
Charge per bunch	1	0.25	0.25	nC
Single bunch repetition rate	120	30	30	Hz
Final linac e^- energy	13.6	13.6	3.5–6.7	GeV
Slice† emittance (injected)	1.2	0.4	0.4	μm
Final projected† emittance	1.5	0.5–1.2	0.5–1.6	μm
Final peak current	3.4	2.5–3.5	0.5–3.5	kA
Timing stability (r.m.s.)	120	50	50	fs
Peak current stability (r.m.s.)	12	8–12	5–10	%
X-rays				
FEL gain length	4.4	3.5	~1.5	m
Radiation wavelength	1.5	1.5	6–22	Å
Photons per pulse	2.0	1.0–2.3	10–20	10^{12}
Energy in X-ray pulse	1.5	1.5–3.0	1–2.5	mJ
Peak X-ray power	10	15–40	3–35	GW
Pulse length (FWHM)	200	70–100	70–500	fs
Bandwidth (FWHM)	0.1	0.2–0.5	0.2–1.0	%
Peak brightness (estimated)	8	20	0.3	10^{32} *
Wavelength stability (r.m.s.)	0.2	0.1	0.2	%
Power stability (r.m.s.)	20	5–12	3–10	%

*Brightness is photons per phase space volume, or photons s^{-1} mm^{-2} $mrad^{-2}$ per 0.1% spectral bandwidth.
†'Slice' refers to femtosecond-scale time slices and 'projected' to the full time-projected (that is, integrated) emittance of the bunch.

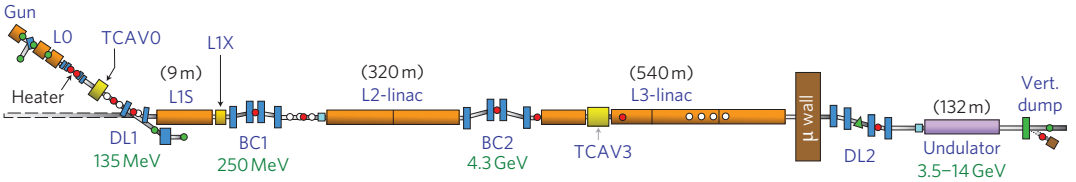

Figure 1 | LCLS machine layout. Layout from the electron gun to the main dump, with two bunch compressors, BC1 and BC2, and a 132-m-long undulator.

The LCLS electron accelerator is based on the last kilometre of the SLAC 3-km-long linac. This remarkable 42-year-old machine[22] uses radiofrequency (RF) fields at 2,856 MHz (S-band) to accelerate electrons up to 50 GeV, most prominently for high-energy physics research. The final kilometre of this linac is now being used to drive the FEL. To create the LCLS, the linac was modified to include a new high-brightness electron injector at the 2 km point, and two magnetic bunch compressor chicanes (BC1 and BC2) were added to increase the peak current of the electron beam in stages, commensurate with the increasing beam energy. A new 350-m-long transport line was built at the end of the linac to deliver the 3.5–15 GeV electrons to the 132-m-long undulator line, after which the electrons are dumped and the X-ray beam is transported to the X-ray diagnostics, or one of several experimental stations. The facility has been designed to allow future expansion with up to eight undulators and separate X-ray beamlines. The LCLS layout is shown in Fig. 1.

The new injector[23] must produce a very bright electron beam in a single bunch generated at a rate of up to 120 Hz with a charge of 0.25 nC (an empirically improved operating point that performs better than the 1-nC design), a peak current of 35 A, and an r.m.s. energy-normalized emittance of <1 μm in each transverse plane. The injector begins with a photocathode RF gun with a copper cathode illuminated by UV light from a frequency tripled pulse from an amplified Ti:Sapphire laser system. Uniform spatial UV shaping is important to generate the low emittance and is accomplished with a 1.2-mm-diameter over-filled aperture imaged to the cathode. The (less critical) uniform temporal shaping is accomplished by stacking two 3-ps-long (FWHM) Gaussian beams separated by 3 ps.

The pair of new bunch compressors shortens the electron bunch and thereby magnifies the peak current from the injector by a factor of ~100, for a final peak current of up to 3.5 kA at the end of the linac. The high peak current is required to efficiently generate and saturate the shortest X-ray wavelengths. The compressors were designed to minimize the effects of coherent synchrotron radiation[24] (CSR), a process that can degrade the electron beam brightness during the compression process as the very short electron bunch begins to radiate coherently in the chicane bend magnets. The effects of CSR have been measured in both compressors and show reasonably good agreement with available computer modelling codes[25]. The electron bunch length is measured using a transverse RF S-band deflecting cavity[26] ('TCAV3' in Fig. 1), which works like a femtosecond-resolution streak camera for electrons and is capable of resolving bunch lengths as short as 25 fs FWHM.

A special 'laser heater'[27,28] is located in the injector at 135 MeV ('Heater' in Fig. 1). This unique component adds a small level of energy spread (~20 keV r.m.s. before bunch compression) to the electron beam to 'Landau damp' a micro-bunching instability before it potentially breaks up the high-brightness electron beam. The system modulates the energy of the electron bunch using a co-propagating IR-laser (758 nm) in a short undulator (0.5 m), which is enclosed within a four-dipole magnetic chicane. The energy modulation is immediately smeared by the last two magnets of the chicane into an uncorrelated energy spread, which continues to smooth the temporal distribution of the bunch as it passes through the downstream bunch compressors. The heater is the first of its kind in a linac-based FEL and has been shown to be quite effective in suppressing this instability and improving FEL performance[29].

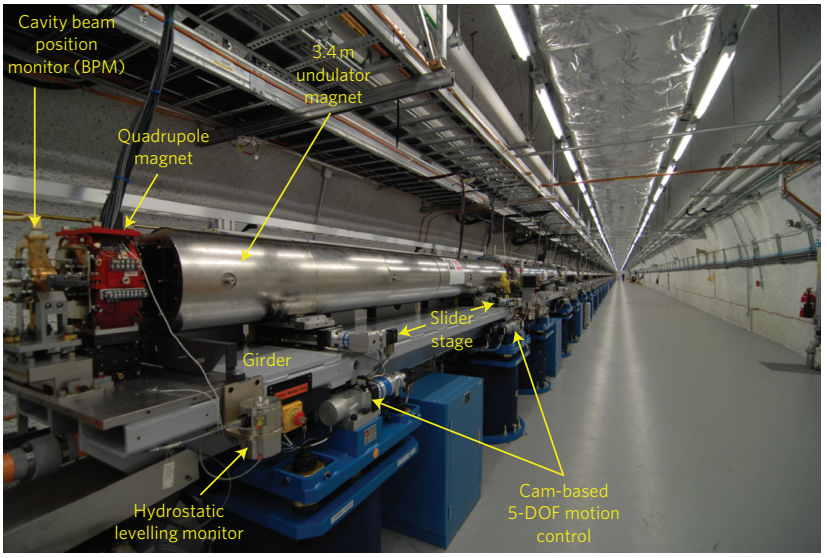

Figure 2 | Photograph of a single undulator segment. The major components are labelled and the space to the right is reserved for a second undulator.

Many beam-stabilizing feedback loops are in operation, with RF-based loops and beam-based loops. The most critical loop uses linac RF phases and voltage levels to control the energy and bunch length (that is, peak current) after each compressor[30]. The bunch length measurements are based on coherent edge radiation from the last dipole magnet of each compressor chicane[31] and are calibrated in amperes of peak current using the transverse RF deflecting cavity. This critical loop maintains the final peak current at any chosen setting from 0.5 to 3.5 kA, as desired, stabilizing the peak current to 5–10% r.m.s. and the final electron energy to $<$0.1% r.m.s. Because the X-ray pulse length is similar to the electron bunch length, the closed-loop control allows the operator to simply enter the desired pulse length into the computer as requested by the user.

Undulator and FEL performance

Undulator. The LCLS undulator system[32] was designed and constructed by Argonne National Laboratory and is 132 m long, including breaks for quadrupole focusing magnets, resulting in 112 m of active undulator. It is composed of thirty-three 3.4-m-long planar, permanent-magnet (neodymium iron boron) undulator segments with a period of 3 cm, full gap height of 6.8 mm (fixed), and undulator magnetic deflection parameter $K = 3.5$ (corresponding to a peak magnetic field of 1.25 T). The undulators and focusing magnets are mounted on cam-based, five-degree-of-freedom (5-DOF), submicrometre controlled horizontal and vertical translation stages (girders) to allow beam-based alignment (see below). Each undulator segment is mounted on the girder through a horizontal slider stage to allow segment retraction (8 cm) to switch off any set of undulators. The undulator magnet poles have canted angles ($\pm$5 mrad) to allow small adjustment of the field (K) to optimize FEL gain for different electron beam parameters, such as energy, peak current and bunch charge.

A 5×12 mm^2 quasi-rectangular vacuum chamber within each segment has a highly polished aluminium surface ($<$0.2 μm finish) to minimize electron beam interactions with rough or resistive chamber walls[33]. Located at each of 33 breaks are a focusing quadrupole magnet, a cavity-type electron beam position monitor (BPM) with a resolution of 0.5 μm, an insertable alignment and beam-size monitoring wire, and a flexible vacuum bellows (see Fig. 2).

To maintain spatial overlap and relative phasing with the X-rays, the electron beam trajectory along the 132-m-long undulator is required to be absolutely straight at the level of ~5 μm r.m.s. over an FEL gain length of ~4 m (at 1.5 Å). With standard beamline survey methods limited to an alignment level of ~50 μm, this extremely challenging requirement is accomplished empirically by recording the electron trajectory (BPM readings) at each of several energy settings (4, 7, 9 and 14 GeV), calculating the displacements needed to correct the alignment and then remotely adjusting the transverse positions of the girders (that is, focusing magnets) to produce a final trajectory that is insensitive to beam energy (that is, dispersion-free)[34]. Examples of final measured trajectories are shown in Fig. 3. In this process, the effects of the Earth's magnetic field can limit the convergence of beam-based alignment, and therefore also the FEL performance, so these weak fields (~0.4 G) must be carefully shielded with μ-metal liners covering each undulator. This beam-based alignment process requires a few hours to accomplish and is repeated every 2–3 weeks as necessary to maintain FEL power. The girder alignment is continuously monitored with submicrometre resolution by a combination of a stretched-wire position monitor system and a hydrostatic levelling system, both permanently installed.

FEL performance. One of the most remarkable aspects of the LCLS start-up was the immediate demonstration of FEL gain on the very first attempt in April 2009. FEL lasing was observed immediately after just 12 (of 33) undulator segments were inserted, and within four days the SASE FEL was fully saturated at the shortest design wavelength of 1.5 Å. The FEL power (at 1.5 Å) as a function of the undulator length is shown in Fig. 4. The relative FEL power is measured for each shot by integrating the intensity measured on an intercepting YAG screen (see Fig. 4 inset) located 50 m downstream of the last undulator segment.

The gain length is obtained through a linear fit to the logarithm of the relative power measurements (30 beam shot averages) versus the location of the last inserted undulator segment. The absolute power values are estimated by scaling to the simulation results from the computer code GENESIS[35], and are in reasonable agreement with independent measurements (10–12 GW at saturation in this early case).

Because the electron peak current (3 kA in Fig. 4) is well calibrated from measurements of the bunch length after BC2 (using 'TCAV3') and the relative electron time-sliced energy spread (0.01% r.m.s.) is controlled by the laser heater, the most uncertain parameter affecting FEL performance is the time-sliced emittance at the end of the linac. Although the measured projected

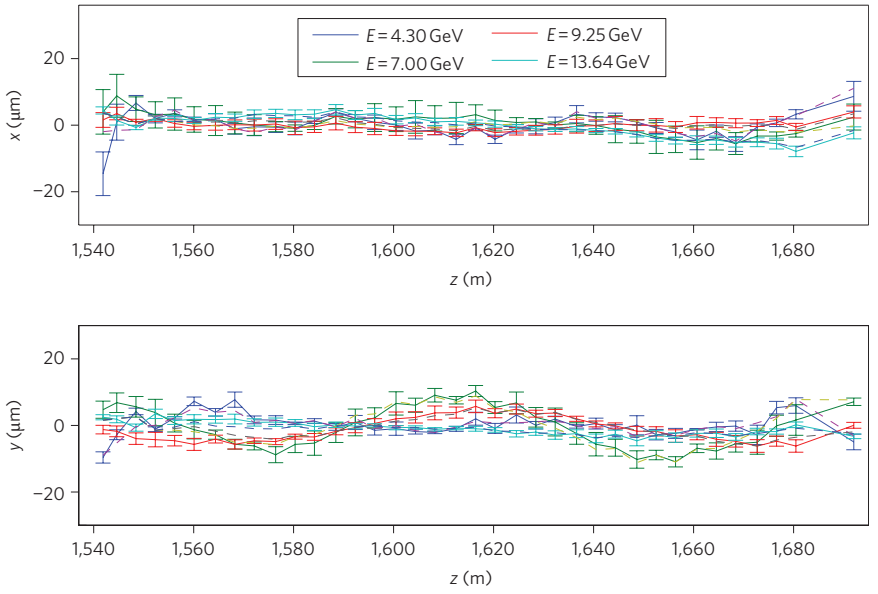

Figure 3 | Electron trajectories through the undulator after beam-based alignment. Both horizontal (top) and vertical (bottom) are shown at four different electron energies (4.3, 7.0, 9.2 and 13.6 GeV). The trajectory is seen to be highly dispersion-free and therefore well aligned. Error bars represent the r.m.s. statistical uncertainty in the measured beam position when averaging 50 beam pulses.

(time-integrated) emittance values there vary from 0.5 to 1.2 μm, most of the emittance growth is thought to be only in the projection (that is, due to transverse centroid shifts along the bunch). The time-sliced emittance measured in the injector (0.4 μm) appears to be well preserved. The figure shows a measured FEL gain length of 3.5 m and a saturation length of 60 m (2/3 of the 90-m design value), consistent with simulation results where the slice emittance is taken as 0.4 μm. The FEL gain length at soft X-ray wavelengths (15 Å) is measured to be ~1.6 m (ref. 36).

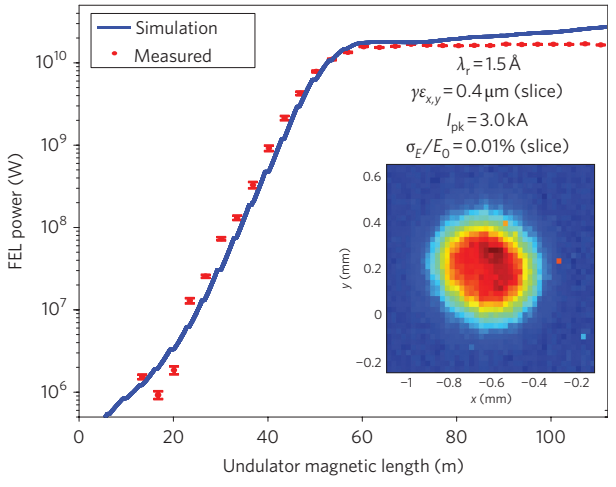

Figure 4 | FEL gain length measurement at 1.5 Å. Measured FEL power (red points) plotted after continuous insertion of each 3.4-m undulator segment showing saturation at 60 m and with all 33 undulator segments installed. Error bars represent the r.m.s. statistical uncertainty in the measured power when averaging 30 beam pulses. The measured gain length is 3.5 m with a GENESIS simulation overlaid (blue curve) and with consistent electron beam parameters shown. The YAG screen image is shown in the inset with 140-μm r.m.s. round X-ray spot size in this early case (April 2009). λ_r is the fundamental FEL radiation wavelength; I_{pk} is the peak current of the electron beam in the undulator; γ is the relativistic Lorentz facotr; $\varepsilon_{x,y}$ is the transverse r.m.s. emittance of the electron beam in the undulator; $\gamma\varepsilon_{x,y}$ is the normalized transverse r.m.s. emittance of the electron beam in the undulator; σ_E/E_0 is the r.m.s. relative energy spread of the electron beam in the undulator (that is, the r.m.s. energy spread, σ_E, divided by the mean electron energy, E_0).

To estimate the total FEL energy in the X-ray pulse, the electron energy loss across the undulator is measured by observing changes of the vertical electron beam position in the dump line after the vertical bend magnets (see Fig. 1), where the momentum dispersion is large. In addition to the FEL process, broadband spontaneous radiation and vacuum chamber wakefields can contribute to energy loss in the undulator. However, these non-FEL effects can be isolated by exciting a large horizontal betatron oscillation in the undulator to suppress the FEL interaction, allowing the FEL-induced energy loss to be precisely determined. This measured average energy loss per electron, multiplied by the electron bunch charge, yields the total energy in the FEL X-ray pulse. Using this method, we consistently measure X-ray pulse energies from 1 to 3 mJ with <5% r.m.s. precision for the nominal 250-pC bunch charge throughout the entire operating wavelength range. This electron-based X-ray energy measurement is also used to calibrate the gas detectors, which measure the relative X-ray pulse energy on each pulse (see below).

Owing to the exceptional electron beam quality and feedback controls, the electron bunch length can easily be varied during FEL operation, especially with soft X-rays (22 to 6 Å). Figure 5 shows the measured X-ray pulse energy at 6 Å (2 keV photon energy) as a function of the electron bunch length (FWHM) over the range between 70 and 350 fs (corresponding to a peak current variation of 3.5–0.7 kA). The X-ray pulse energy increases with bunch length, probably due to reduced collective effects in the bunch compressors and undulator, but rolls off above 250 fs, because the peak current also drops. To estimate the X-ray peak power, we divide the X-ray pulse energy by the X-ray pulse length, which is assumed to be the same as the measured electron bunch length. Figure 5 shows that the X-ray peak power is increased with a shorter pulse length, even where the total pulse energy decreases.

To reach exceptionally short pulse durations, the LCLS has added a low-charge operating mode (20 pC). The reduced bunch charge provides even better transverse emittance from the gun and also mitigates collective effects in the accelerator, allowing for extreme

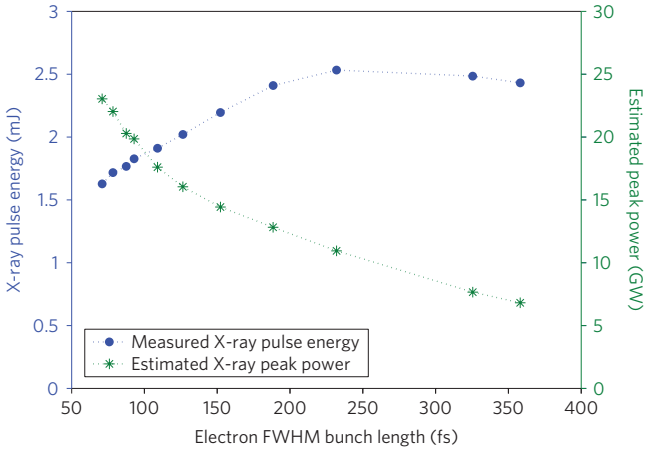

Figure 5 | Measured X-ray pulse energy (blue) and estimated peak power (green) versus FWHM electron bunch length. Both are shown for 2 keV photons and with a constant 250-pC electron bunch charge.

bunch compression. The compressed electron bunch length is estimated to be less than 10 fs FWHM and is too short to be measured with the transverse deflecting cavity. Stable saturated FEL operations with estimated power levels similar to Fig. 5 have been routinely achieved over the entire LCLS wavelength range. This new ultrashort pulse mode is now being delivered to a host of researchers.

X-ray diagnostics and optics

The primary X-ray diagnostics, designed and fabricated by the Lawrence Livermore National Laboratory, are located downstream of the electron dump in a 40-m tunnel called the Front End Enclosure (FEE). The diagnostics occupy the upstream half of the FEE and have an unrestricted view of the FEL beam and the surrounding spontaneous radiation halo. The adjustable low- and high-energy mirror systems[37] occupy the downstream half of the FEE, directing soft X-rays into two of the experimental stations and hard X-rays into the other four stations.

Although the average X-ray power produced by LCLS is quite modest ($<$1 W), the peak power is extremely high (up to 40 GW). This presents unusual problems for the X-ray beam containment, shielding and optical elements. The thermal loads are negligible, so in most cases no special cooling is needed. However, the peak power levels are so high and the beam is so concentrated that local damage is likely for most materials placed in the beam. The absorbed energy simply cannot escape the exposed volume fast enough and local temperatures can exceed the melting threshold for the absorber material. Therefore, at LCLS the FEL beam path is very carefully controlled by a series of special collimators. The collimators, beam stoppers and all shutters include several millimetres of boron carbide protecting their upstream faces. The combination of a low absorption coefficient for X-rays and a high melting point allow boron carbide to safely intercept the unfocused FEL beam. Even boron carbide would be at risk if the FEL beam were concentrated, so the first LCLS X-ray shutters are located nearly 50 m downstream of the undulator[38].

The X-ray optics and diagnostics in the FEE include absorbers, imagers and intensity measuring devices. The absorber section includes both insertable solid attenuators, useful at hard-X-ray energies, and a gas absorber useful for soft X-rays. The solid and gas attenuators can be used individually or together to provide attenuation of at least three orders of magnitude across the full design wavelength range of LCLS. The gas absorber consists of a 4-m pipe that can be filled with nitrogen gas at a controlled low pressure (up to 10 torr). The gas absorber is flanked by differential pumping stages, so that no windows are needed.

Located upstream and downstream of the absorber section are pulse-energy detectors that rely on absorption of X-rays in low-pressure nitrogen gas. The energy absorbed in the gas excites the nitrogen molecules, leading to UV fluorescence, which is detected by photomultiplier tubes. These 'gas detectors' measure FEL pulse energies in the microjoule to millijoule range[39]. The detectors are nearly transparent and are used for pulse-by-pulse monitoring of the FEL intensity. An additional pulse-energy detector can be inserted to allow accurate calibration of the gas detectors. This detector is not transparent and relies on careful calorimetry of the heat pulse deposited in a silicon absorber by the FEL X-rays[40].

The downstream half of the FEE is occupied by an X-ray beam switchyard based on grazing-incidence mirrors. In addition to directing the FEL beam to the various experimental stations, the mirrors serve as low-pass filters which separate the FEL radiation from higher-energy spontaneous undulator radiation and Bremsstrahlung background radiation. This high-energy radiation is prevented from reaching the experimental stations, simplifying their shielding requirements. Two mirror systems are used: a soft-X-ray mirror system with reflectivity cut-off at 2 keV, and a hard-X-ray mirror system with cut-off at 25 keV. Moving the first soft-X-ray mirror into the beam directs it to one of two soft-X-ray experimental stations. Moving the first soft-X-ray mirror out of the beam allows it to intercept two hard-X-ray mirrors arranged in a periscope geometry and thence to several hard-X-ray experimental stations. The soft-X-ray mirrors are coated with boron carbide and the hard-X-ray mirrors with silicon carbide, which is slightly denser.

The mirrors were carefully polished to extreme flatness to preserve the coherent FEL wavefront. Visible-light interferometry and atomic-force microscopy were used to characterize the surfaces of the single-crystal silicon mirror substrates at a wide range of spatial frequencies. In some cases, ion-beam etching was used to improve the surface figure based on the metrology. The resulting mirrors satisfy the Marechal criterion for preservation of X-ray wavefronts throughout the LCLS design range[41,42].

Operational experience

The LCLS is presently operated for users 120 h per week, with the remaining time for machine development and maintenance. Only the AMO (atomic, molecular and optical science) soft-X-ray hutch was in operation at the time this article was written (December 2009), with the SXR (soft-X-ray research) hutch ready for commissioning in May 2010, and four more hard-X-ray hutches opening by 2012.

Machine reliability has been exceptional in this first run, with 97% of scheduled time available. In addition, overall stability has been quite good, as partially listed in Table 1. The FEL power stability depends on the peak current setting and X-ray wavelength. With soft X-rays (usually $<$2 kA, and the FEL power deep into saturation) the total energy in the pulse is stable to 3–5% r.m.s. over $\sim$1 min at 30 Hz. With hard X-rays (usually 3-kA peak current) the FEL power is less stable due to the more aggressive electron beam compression, with 5–12% r.m.s. variations. Stability over longer timescales is not greatly different, because feedback loops maintain the electron peak current, energy and trajectory.

The transverse pointing stability of the X-ray beam also depends on the desired FEL wavelength (that is, the electron energy), where hard X-rays show an r.m.s. variation of their centroid position at 10–20% of their r.m.s. beam size (a transverse position jitter of $\sim$20 μm r.m.s. at the FEE imager). These levels can increase to 30% with soft X-rays (lower and more sensitive electron energy).

First science and future improvements

First science opportunities at the LCLS have concentrated on strong field and short pulse phenomena in atoms, small molecules and

clusters, as well as on X-ray imaging of nanoscale materials, with radiation in the range 6–15 Å. The beamline has a Kirkpatrick–Baez mirror pair capable of producing a focused beam of 1–3 μm in diameter, leading to a focused single-pulse fluence of up to 1×10^{21} photons cm^{-2} and intensities reaching 1×10^{18} W cm^{-2}. The data are currently under analysis by the ten experimental teams involved in the first run and detailed science results are forthcoming.

First experiments have already verified that the focused LCLS beam is capable of producing very high-order atomic charge states. Therefore complex chains of rapid sequential photoionization and competing Auger relaxation can be studied. The early success in reducing the pulse length to less than 10 fs (based on computer simulations and indirect measurements only; see ref. 22), has opened up new research opportunities to study transient states as well.

Timing between the X-rays and a comparably short pulse optical laser has been commissioned, with timing uncertainty on the scale of the X-ray pulse duration, opening the door for pump–probe experiments between conventional lasers and LCLS X-rays. Imaging experiments have shown that high-quality diffraction images can be recorded with just one LCLS X-ray pulse on a single nanoscale object.

With the rapid and striking success of the LCLS, the X-ray fourth-generation light source has become a reality. The routine and stable operation of such a challenging machine generates great optimism regarding future efforts worldwide using more aggressive designs with outstanding scientific potential.

Efforts are already under way to upgrade the LCLS, extending the wavelength range down to 0.5 Å, by modifying the present undulator, and also up to 60 Å, by building a new soft-X-ray undulator parallel to the existing one. Diverse new features will be included, such as self-seeding to narrow the FEL bandwidth[43] two-pulse-two-colour X-ray generation with variable delay, full X-ray polarization control, and external laser-based seeding using the new idea of 'echo-enabled' harmonic generation[44], ultimately providing a very wide spectrum of X-rays with superior gain, bandwidth, coherence and pulse length control.

Received 16 April 2010; accepted 21 June 2010;
published online 1 August 2010

References

1. Leone, S. R. Report of the Basic Energy Sciences Advisory Committee Panel on Novel Coherent Light Sources. U.S. Department of Energy, January 1999. http://www.er.doe.gov/production/bes/BESAC/ncls_rep.PDF.
2. Madey, J. Stimulated emission of bremsstrahlung in a periodic magnetic field. *J. Appl. Phys.* **42,** 1906–1913 (1971).
3. Kondratenko, K. & Saldin, E. Generating of coherent radiation by a relativistic electron beam in an ondulator. *Part. Accel.* **10,** 207–216 (1980).
4. Bonifacio, R., Pellegrini, C. & Narducci, L. M. Collective instabilities and high-gain regime in a free electron laser. *Opt. Commun.* **50,** 373–378 (1984).
5. Huang, Z. & Kim, K.-J. Review of X-ray free-electron laser theory. *Phys. Rev. ST Accel. Beams* **10,** 034801 (2007).
6. Winick, H. The linac coherent light source (LCLS): a fourth-generation light source using the SLAC linac. *J. Elec. Spec. Rel. Phenom.* **75,** 1–8 (1995).
7. Arthur, J. *et al.* Linac Coherent Light Source (LCLS) Conceptual Design Report. SLAC-R-593 (Stanford 2002) (see also http://ssrl.slac.stanford.edu/lcls/CDR/).
8. Pellegrini, C. A 4 to 0.1 nm FEL based on the SLAC linac, in Workshop *on 4th Generation Light Sources* SSRL-Report-92/02 (eds Cornacchia, M. & Winnick, H.) 364–375 (SSL, 1992).
9. Arthur, J., Materlick, G. & Winick, H. The LCLS: A fourth generation light source using the SLAC linac. *Rev. Sci. Instrum.* **66,** 1987–1989 (1995).
10. Neutze, R., Wouts, R., Van Der Spoel, D., Weckert, E. & Hajdu, J. Potential for biomolecular imaging with femtosecond X-ray pulses. *Nature* **406,** 752–757 (2000).
11. Hogan, M. *et al.* Measurements of gain larger than 105 at 12 μm in a self-amplified spontaneous-emission free-electron laser. *Phys. Rev. Lett.* **81,** 4867–4870 (1998).
12. Andruszkow, J. *et al.* First observation of self-amplified spontaneous emission in a free-electron laser at 109 nm wavelength. *Phys. Rev. Lett.* **85,** 3825–3829 (2000).
13. Milton, S. *et al.* Exponential gain and saturation of a self-amplified spontaneous emission free-electron laser. *Science* **292,** 2037–2041 (2001).
14. Ayvazyan, V. *et al.* Generation of GW radiation pulses from a VUV free-electron laser operating in the femtosecond regime. *Phys. Rev. Lett.* **88,** 104802 (2002).
15. Tremaine, A. *et al.* Experimental characterization of nonlinear harmonic radiation from a visible self-amplified spontaneous emission free-electron laser at saturation. *Phys. Rev. Lett.* **88,** 204801 (2002).
16. Shintake, T. *et al.* A compact free-electron laser for generating coherent radiation in the extreme ultraviolet region. *Nature Photon.* **2,** 555–559 (2008).
17. Ackermann, W. *et al.* Operation of a free-electron laser from the extreme ultraviolet to the water window. *Nature Photon.* **1,** 336–342 (2007).
18. Altarelli, M. *et al.* (eds). XFEL: The European X-Ray Free-Electron Laser Technical Design Report. Preprint DESY 2006-097 (DESY, 2006) (see also http://xfel.desy.de).
19. Tanaka, T. & Shintake, T. (eds) SCSS XFEL Conceptual Design Report (Riken Harima Institute, 2005) (see also http://www-xfel.spring8.or.jp).
20. Patterson, B. D. *et al.* Coherent science at the SwissFEL X-ray Laser. *New J. Phys.* **12,** 035012 (2010) (see also http://fel.web.psi.ch/).
21. Ding, Y. *et al.* Measurements and simulations of ultralow emittance and ultrashort electron beams in the linac coherent light source. *Phys. Rev. Lett.* **102,** 254801 (2009).
22. Neal, R. B. *The Stanford Two-Mile Accelerator* (W.A. Benjamin, 1968).
23. Akre, R. *et al.* Commissioning the Linac Coherent Light Source injector. *Phys. Rev. ST Accel. Beams* **11,** 030703 (2008).
24. Saldin, E., Schneidmiller, E. & Yurkov, M. Coherent radiation of an electron bunch moving in an arc of a circle. *Proc. 1997 Part. Accel. Conf.*, 12–16 May 1997, Vancouver, BC, Canada, 1658–1660 (IEEE, 1997).
25. Bane, K. *et al.* Measurements and modelling of coherent synchrotron radiation and its impact on the Linac Coherent Light Source electron beam. *Phys. Rev. ST Accel. Beams* **12,** 030704 (2009).
26. Akre, R. *et al.* A transverse RF deflecting structure for bunch length and phase space diagnostics. *Proc. 2001 Part. Accel. Conf.*, 18–22 June 2001, Chicago, IL, USA, 2353–2355 (IEEE, 2001).
27. Saldin, E., Schneidmiller, E. & Yurkov, M. Longitudinal space charge-driven microbunching instability in the TESLA test facility linac. *Nucl. Instrum. Meth. A* **528,** 355–359 (2004).
28. Huang, Z. *et al.* Suppression of microbunching instability in the linac coherent light source. *Phys. Rev. ST Accel. Beams* **7,** 074401 (2004).
29. Huang, Z. *et al.* Measurements of the linac coherent light source laser heater and its impact on the X-ray free-electron laser performance. *Phys. Rev. ST Accel. Beams* **13,** 020703 (2010).
30. Wu, J. *et al.* Commissioning experience with the linac coherent light source feedback systems. *Proc. of the 2008 Free-Electron Laser Conference*, 24–29 August 2008, Gyeongju, Korea, p. 98–101 (IEEE, 2008).
31. Loos, H., Borden, T., Emma, P., Frisch, J. & Wu, J. Relative bunch length monitor for the linac coherent light source (LCLS) using coherent edge radiation. *Proc. of the 2007 Part. Accel. Conference*, 25–29 June 2007, Albuquerque, NM, USA, p. 4189–4191 (IEEE, 2007).
32. Nuhn, H.-D. LCLS undulator commissioning, alignment, and performance. *Proc. of the 2009 Free-Electron Laser Conference*, 23–28 August 2009, Liverpool, UK, p. 714–721 (JACOW, 2009).
33. Bane, K. L. F. & Stupakov, G. Resistive wall wakefield in the LCLS undulator. *Proc. of the 2005 Part. Accel. Conference*, 16–20 May 2005, Knoxville, TN, USA, p. 3390–3392 (IEEE, 2005).
34. Emma, P., Carr, R. & Nuhn, H.-D. Beam based alignment for the LCLS FEL undulator. *Nucl. Instrum. Methods A* **429,** 407–413 (1999).
35. Reiche, S. GENESIS 1.3: a fully 3D time-dependent FEL simulation code. *Nucl. Instrum. Methods A* **429,** 243–248 (1999).
36. Ratner, D. *et al.* FEL gain length and taper measurements at LCLS. *Proc. of the 2009 Free-Electron Laser Conference*, 23–28 August 2009, Liverpool, UK, p. 221–224 (JACOW, 2009).
37. McCarville, T. J. *et al.* Opto-mechanical design considerations for the Linac Coherent Light Source X-ray mirror system. *Proc. SPIE* **7077,** 70770E (2008).
38. Hau-Riege, S. P. *et al.* Wavelength dependence of the damage threshold of inorganic materials under extreme-ultraviolet free-electron-laser irradiation. *Appl. Phys. Lett.* **95,** 111104 (2009).
39. Hau-Riege, S. P., Bionta, R. M., Ryutov, D. D. & Krzywinski, J. Measurement of free-electron laser pulse energies by photoluminescence in nitrogen gas. *J. Appl. Phys.* **103,** 053306 (2008).
40. Yong, G. J. *et al.* Collassal magnetoresistive manganite based fast bolometric X-ray sensors for total energy measurements of free electron lasers. *Sensor Lett.* **6,** 741–745 (2008).
41. Barty, A. *et al.* Predicting the coherent X-ray wavefront focal properties at the Linac Coherent Light Source (LCLS) X-ray free electron laser. *Opt. Express* **17,** 15508–15519 (2009).
42. Soufli, R. *et al.* Morphology, microstructure, stress and damage properties of thin film coatings for the LCLS X-ray mirrors. *Proc. SPIE* **7361,** 73610U (2009).
43. Feldhaus, J. *et al.* Possible application of X-ray optical elements for reducing the spectral bandwidth of an X-ray SASE FEL. *Opt. Commun.* **140,** 341–352 (1997).

44. Stupakov, G. Using the beam-echo effect for generation of short-wavelength radiation. *Phys. Rev. Lett.* **102,** 074801 (2009).

Acknowledgements
The authors would like to express their sincere thanks to the many people at SLAC, LLNL, ANL and UCLA who contributed to this project, including the accelerator operations group, the electron and X-ray systems controls groups, ANL undulator systems design, LLNL X-ray diagnostics/optics, RF engineering, mechanical design, metrology, precision magnetic measurements, power conversion and the dedicated machine maintenance groups. We also thank the LBNL timing and synchronization team and in particular H. Sinn and J. Gruenert of DESY and S. Zholents of LBNL for their appreciable help with FEL commissioning in the spring of 2009. We are also grateful for the support of the US Department of Energy, Office of Science, under contract no. DE-AC02-76SF005, and the sponsorship of the LCLS mission by the Office of Basic Energy Sciences.

Author contributions
P.E., J.A., R.B., P.B., Z.H. and H.-D.N. co-wrote the paper. All authors designed, constructed and tested the accelerator and X-ray systems, performed experiments and analysed the data. J.G. was the LCLS project director.

Additional information
The authors declare no competing financial interests. Reprints and permission information is available online at http://npg.nature.com/reprintsandpermissions/. Correspondence and requests for materials should be addressed to P.E.